25.10.2024

D2.4 Validation of Temperature and Humidity in a Greenhouse Environment using CFD

THEGREEFA

Thermochemical fluids in greenhouse farming

This project has received funding from the European Union's Horizon 2020 research and innovation program under grant agreement 101000801.

Document references

Project Acronym	**TheGreefa**
Project Title	**Thermochemical fluids in greenhouse farming**
Project Coordinator	**Serena Danesi (ZHAW)**
Project Duration	**October 2020 – September 2023 (36 months)**

Deliverable No./Title	**D2.4 Validation of Temperature and Humidity in a Greenhouse Environment using CFD**
Dissemination level [1]	
Work Package	**WP2 – Modelling and control**
Task	**Task 2.1: CFD simulations for greenhouse concept**
Lead beneficiary	David Dudli (ZHAW)
Contributing beneficiary(ies)	Marius Banica (ZHAW), Serena Danesi (ZHAW)
Due date of deliverable	**31/05/2024**
Actual submission date	**31/05/2024**

[1] PU = Public
PP = Restricted to other programme participants (including the Commission Services)
RE = Restricted to a group specified by the consortium (including the Commission Services)
CO = Confidential, only for members of the consortium (including the Commission Services)

Document history

V	Date	Beneficiary	Short description of contents and/or changes
V0	31/05/2024	David Dudli (ZHAW)	First release
V01	25/10/2024	Marius Banica (ZHAW)	More details on page 8 and 11.

This project has received funding from the European Union's Horizon 2020 research and innovation program under grant agreement 101000801.

Executive Summary

This report builds upon the existing work "D2.1 CFD Simulation in Greenhouse Farming" and is part of WP2 - Modelling and Control in TheGreefa project. It describes the development of the CFD model mentioned to predict the microclimate in a greenhouse. The previous scope of using this model to identify suitable sensor positions and locations for air conditioning units is no longer pursued. Instead, this study focuses on the modelling of radiation and humidity. In contrast to the previous report, these complex phenomena can also be validated with measurement data from an experimental greenhouse in Chorfech, Tunisia. Due to these new circumstances, some findings from the simulation for the Wädenswil greenhouse are no longer applicable.

The introduction picks up the status of the previous report and explains the different starting position in more detail. The theoretical backgrounds for density and turbulence modelling are not examined as they have already been dealt with. The methodology for modelling radiation and humidity and its applicability for the greenhouse is comprehensively explained, justifying the selection of the Solar Load Model for the radiation and the Species Transport model for humidity. Section 3 describes the experimental greenhouse near Tunis and the measurements collected in June 2023 by Chaibi M. Thameur. The geometry, material properties and climate conditions of the greenhouse are documented, leading to the choice of two design points on 16 June 2023 at 4:00 AM and 1:00 PM. These are then used in Section 4 to implement two steady state CFD models, one with symmetry simplifications and another with the full greenhouse domain. The climate data of the chosen cool and warm extrema is used to derive two sets of adequate boundary conditions.

The CFD models feature two boundaries: the greenhouse floor and cover. The buoyancy-driven flow occurs due to marginal density differences that are computed using the Boussinesq Approximation. The heat transfer across boundaries is implemented with estimated convection coefficients. For the warm design point, the radiation acts as a considerable energy source, whereas for the cool design point, only the temperature difference between the floor and the ambient account for fluid motion. Crop activity is not considered as no data is available.

The model developed indicates that the influence of crops must be considered, as soil temperatures rise above 100°C near the ground when using the solar load model. Furthermore, latent heat flows due to condensation/evaporation must also be accounted for, as a relative humidity partially rises above 100% on the floor at 4:00 AM. Nevertheless, the residual convergence is excellent, and the energy imbalance stagnates at 2.8%, reflecting these findings.

The construction of a model that depicts the activity of crops and condensation phenomena is of paramount importance for the achievement of accurate model predictions. Although this remains the subject of further investigation, a suitable model for humidity and radiation was identified, which will facilitate further development.

This project has received funding from the European Union's Horizon 2020 research and innovation program under grant agreement 101000801.

Table of Contents

This project has received funding from the European Union's Horizon 2020 research and innovation program under grant agreement 101000801.

List of Figures

List of Tables

This project has received funding from the European Union's Horizon 2020 research and innovation program under grant agreement 101000801.

1. Introduction

The modeling of greenhouses is a common problem, as the number of scientific publications shows. In addition to the simpler approach of balancing the heat flows, CFD (Computational Fluid Dynamics) is a valuable tool that is increasingly used (Abid et al., 2023). This approach is useful for modeling the microclimate of interest. The main physical variables that influence the climate in the greenhouse are described in the introduction to the report "D2.1 CFD Simulation in Greenhouse Farming". In this presented work, two CFD models were also developed for a test greenhouse in Wädenswil, Switzerland, focusing on the use for microclimate control and the identification of suitable positions for sensors and air conditioning technology. The modeling of turbulence and marginal density fluctuations is also described in detail.

This work builds on upon this report and introduces humidity with the species transport model. Furthermore, a radiation model better adapted to the problem is implemented. With the climate measurement data now available from a test greenhouse near Tunis, it is possible to validate the applicability and limits of the models.

2. Theoretical Background and Models

The modelling of density and turbulence with ANSYS Fluent is being continued from the previous work. The concepts for natural convection modelling and the impact of the material properties, radiation, and humidity are assessed as they apply to this work.

a. Natural Convection Modelling

Natural convection occurs wherever a fluid moves by natural means, such as buoyancy. When air near a greenhouse surface (such as the ground or plants) is heated, it becomes less dense and rises. Cooler, denser air then replaces it, creating a convective loop. In Fluent, the natural convection of humid air is modeled by solving the Navier-Stokes equations. The continuity equation (1) ensures mass conservation, and the momentum equation (2) includes the buoyancy term to account for natural convection (ANSYS, 2023, Section 1.2). The variables are: ρ is the fluid density, $\vec{U}$ the flow velocity, p the pressure, μ the viscosity, and $\vec{g}$ the gravitational acceleration.

$$\frac{\partial \rho}{\partial t} + \nabla \cdot (\rho \vec{U}) = 0 \tag{1}$$

$$\frac{\partial (\rho \vec{U})}{\partial t} + \nabla \cdot (\rho \vec{U} \vec{U}) = -\nabla p + \nabla \cdot (\mu \nabla \vec{U}) + \rho \vec{g} \tag{2}$$

For thermal modeling such as natural convection, these equations are coupled with the energy equation (3) that describes the heat transfer within the fluid:

$$\frac{\partial}{\partial t}\left(\rho\left(E + \frac{U^2}{2}\right)\right) + \nabla \cdot \left(\rho \vec{U}\left(h + \frac{U^2}{2}\right)\right) = \nabla \cdot \left(\lambda \nabla T - \sum_i h_i \vec{J}_i\right) + S_h \tag{3}$$

where E is the energy, h ist the enthalpy, T is the temperature, $\vec{J}_i$ the diffusion flux of species i, and S_h the source term for heat, such as radiation or chemical reactions (ANSYS, 2023, Section 5.2.1).

The energy equation mainly depends on the definition of material properties. In a flow as it occurs in a greenhouse at atmosphere pressure, several material properties are solely temperature sensitive. The value variation of air and water vapor is illustrated in **Figure 1**. Even if the water vapor mass fraction

This project has received funding from the European Union's Horizon 2020 research and innovation program under grant agreement 101000801.

in a species mixture is very small, its impact on the thermal properties is considerable (Wierenga et al., 1969). Therefore, the mixture model is also a sensitive choice that carefully considered when modeling humid air.

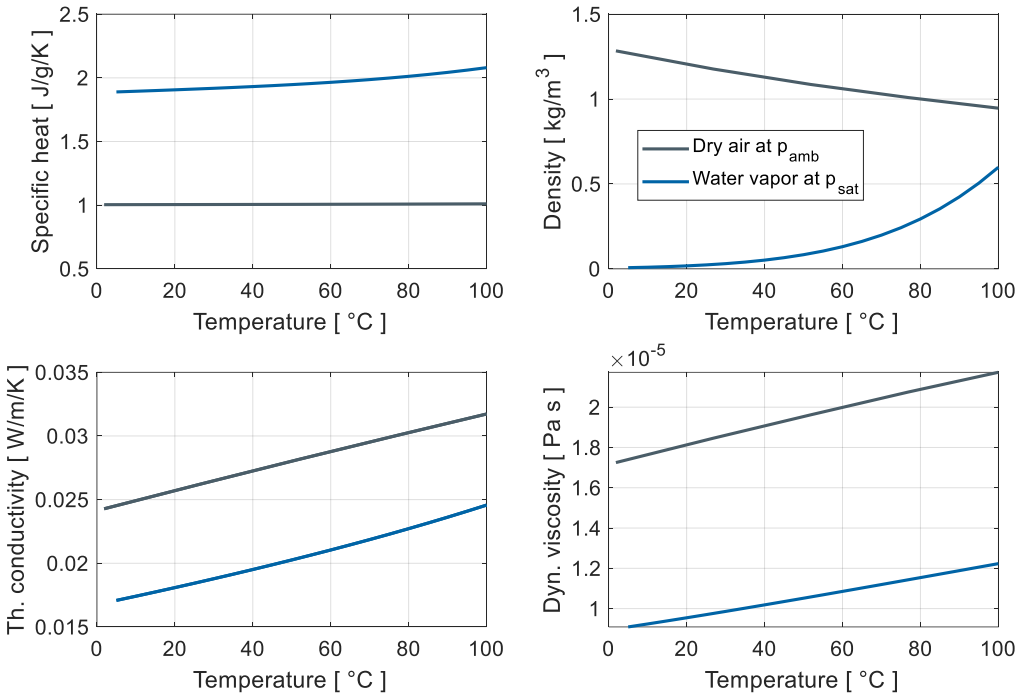

Figure 1 - Temperature dependent thermal properties of dry air at ambient pressure ($1.0132 \cdot 10^5$Pa) and water vapor at saturation pressure. Upper left to lower right: Specific heat capacity c_p, density ρ, thermal conductivity λ, and dynamic viscosity η. The data of air was collected from "Wärmeübertragung" (engl. "Heat Transfer") (Walter Wagner, 1998), the data for water vapor from the public NIST database (National Institute of Standards and Technology (NIST), 2023).

As the conservation equations (1-3) indicate, the material properties strongly affect continuity, momentum, and energy balances. Thus, constant values might not be sufficient in all cases, making it essential to use a temperature dependent model.

- Variations of the density ρ trigger buoyancy-driven flows. An accurate local value for this property is crucial to predict natural convection flows.
- The specific heat capacity c_p affects how quickly the air can absorb heat, influencing the thermal inertia and thus the development of temperature gradients.
- The thermal conductivity λ determines the rate at which heat diffuses through the air. Low thermal conductivity enhances localized heating, strengthening buoyant forces.
- The viscosity η of the air affects the flow resistance. Low viscosity allows for more vigorous convection, enhancing the mixing and redistribution of heat.

This project has received funding from the European Union's Horizon 2020 research and innovation program under grant agreement 101000801.

b. Radiation Modelling

Radiation modelling is of paramount importance in the simulation of greenhouse environments. ANSYS Fluent provides several radiation models to capture the complexities of radiative heat transfer. There are six primary radiation models available in Fluent, all of which take a different approach at solving the radiative transfer equation (RTE) described in the Fluent Theory Guide (ANSYS, 2023, Section 5.3.2):

- **Discrete Ordinates (DO) Model**: This model solves RTE the for a finite number of discrete solid angles, providing a detailed and accurate description of radiation in participating media.
- **P-1 Model**: Based on the spherical harmonics method, the P-1 model is simpler and computationally less intensive than the DO model. It approximates the RTE by using the first few terms of the spherical harmonics series.
- **Surface-to-Surface (S2S) Model**: This model is used for systems where radiation exchange occurs primarily between surfaces, neglecting the effect of the medium between them.
- **Rosseland Model**: Suitable for optically thick media, the Rosseland model simplifies the RTE by using diffusion approximation.
- **Discrete Transfer Radiation Model (DTRM)**: This model traces rays from surfaces, considering the interactions of these rays with the medium.
- **Monte Carlo (MC) Model**: The MC model simulates radiation by probabilistically tracking a large number of photons as they interact with the environment. It offers high accuracy by generating photon histories but is computationally expensive.

While the aforementioned radiation models are robust for many industrial and engineering applications, they present certain limitations when applied to simulating the thermal environment within a greenhouse. Rosseland and p-1 are not suited for optically thin problems, S2S does not account for multiband radiation, and the others are generally resource-heavy and yield results too detailed for the specific problem under investigation.

A different approach is to model radiative heat transfer with the **Solar Load Model**, described in the Fluent User's Guide (ANSYS, 2023b, Section 15.3.11.2). It is perfectly suited for the task at hand, providing a simple and yet efficient way to cover the specific needs of greenhouse modeling. It is tailored to account for the direct and diffuse solar radiation incident on a structure. Key features of the Solar Load Model include:

- The model considers the directional dependence of the sun relative to the greenhouse, adjusting the radiation intensity and angle accordingly.
- It incorporates spectral properties of greenhouse materials by dividing the radiation into a visible and an infrared band. This ensures more accurate simulation of the solar energy that penetrates the greenhouse.
- Prior to solving, a face-by-face shade analysis is performed in order to account for drop shadows of opaque bodies, and primary reflections of the incident load are calculated.
- The Solar Load Model supports transient simulations, allowing for the analysis of time-dependent variations in solar radiation and their effects on the greenhouse environment.

It is observed that this model does not account for spectral scattering within the transmitting medium. Consequently, it is classified as a "non-participating" model. However, this does not diminish the applicability of this model for the greenhouse problem, as humid air can be regarded as transparent (Fenn et al., 1981). For our simulations, this means that propagation of radiation in the computational

This project has received funding from the European Union's Horizon 2020 research and innovation program under grant agreement 101000801.

domain was neglected, and the solar model was only used to provide appropriate heat fluxes at the boundaries.A

c. Humidity Modelling

In order to model the humidity correctly, it is common to define a gas mixture of dry air and water vapor (Malekjani & Jafari, 2018). Fluent recommends the **Species Transport Model** without chemical reactions in the Theory Guide (ANSYS, 2023a, Section 7.1). This model is a powerful tool for simulating mixtures of different chemical species, particularly suitable for applications that analyze the transport and distribution of mixed gases in a medium. For the application of a greenhouse with humid air (without condensation/evaporation phenomena), this model can be used to study the behavior of humid air.

The Species Transport Model is based on the solution of the transport equations for each individual chemical species (4) in a multi-component gas mixture. These equations describe the change in concentration of a species due to convection, diffusion, and possible sources/sinks. While the assumption of equal diffusivities is problematic for laminar flows, it is generally acceptable for turbulent flows where turbulent convection overwhelms molecular diffusion. The (density-averaged) mixture fraction equation is for species i is

$$\frac{\partial}{\partial t}(\rho\, Y_i) + \nabla \cdot \left(\rho \vec{U} Y_i\right) = \nabla \cdot \left(\left(\frac{\lambda}{c_p} + \frac{\mu_t}{Pr_t}\right) \nabla \mathrm{Y_i}\right) + R_i + S_i \qquad (4)$$

where ρ is the mixture density, Y_i the mass fraction of species i, $\vec{U}$ the flow velocity, λ the laminar thermal conductivity, c_p the mixture specific heat, μ_t the turbulent viscosity, Pr_t the turbulent Prandtl number, and R_i/S_i the reaction/source terms of species i (ANSYS, 2023a, Section 8.1.2.1.2).

3. Chorfech Experimental Greenhouse

The CFD model under development is intended to predict the thermophysical conditions in a greenhouse in Chorfech, Sidi Thabet, Tunisia. The following sections describe the measured microclimate data in order to derive adequate boundary conditions and validation criteria. The data, along with basic geometric information, was kindly provided by Chaibi M. Thameur as part of TheGreefa project. Values for defining relevant soil and cover material properties were also provided.

a. Geometry

The greenhouse is built with nine semi-circular arches with a height of 4.5m, each of which adjoins two lower arches with a height of 3.8m. This creates nine ribs shaped according to the bellows principle, shown in **Figure 2**. The total length between the outermost large arches is 10.5m, which suggests a rib spacing of 1.3125m. The smaller buildings in front of the structure are neglected for the scope of this work, which is why the dimensions are not given. Inside the greenhouse, in addition to short plants, there are air conditioning systems and support structures as shown in **Figure 3**. The central axis of the greenhouse is oriented 40° from north to east. It is located in Chorfech, Sidi Thabet, around 20km outside Tunis. The solar data was selected for 36.94 °E longitude and 10.04 °N latitude in the GMT+1 time zone.

This project has received funding from the European Union's Horizon 2020 research and innovation program under grant agreement 101000801.

Figure 2 - The greenhouse is unshaded and consists of nine semi-cylindrical ribs.

Figure 3 - The inside of the greenhouse contains crops, air conditioning systems and support structures.

b. Properties of Soil and Cover Material

The soils mineralogy was assessed at the greenhouse and shows the constituents in **Table 1**. The contents of sand are negligible at all layer depths and rarely exceed 0.6%.

Table 1 - Soil components at the greenhouse site in different layers

Soil layer [-cm]	**Clay** [%]	**Silt** [%]	**Others** [%]
0-20	37.4	33.8	28.8
20-40	37.4	34.8	27.8
40-80	32.4	34.6	33.0
80-120	26.6	30.7	42.7
120-150	33.4	31.6	35.0

The thermal properties of soil are challenging to determine due to the significant influence of water content in addition to its mineral composition (Ochsner, 2017). Assuming a volumetric water content

This project has received funding from the European Union's Horizon 2020 research and innovation program under grant agreement 101000801.

of 10%, material properties were estimated using (Abu-Hamdeh, 2003). The specific heat capacity was estimated to be around 1700 J/kg/K, the thermal conductivity at 1 W/m/K, and the density 1300 kg/m³.

The cover material is a plastic foil with a thickness of 180µm. Its optical properties are measured for visible (400…700 nm) and infrared (IR at 7…13µm) wavelengths after thoroughly removing any anti-drip, yielding:

- Visible transmission 88.5±0.5%
- Visible diffusion 45±2%
- IR transmission <18%

For the used material, since the propagation of radiation in the computational domain was neglected, refraction and extinction played no role in these models, and the associated coefficients did not have to be prescribed. However, the transmission coefficients in the visible and the IR bands are provided here for the cover. The boundary conditions are also described in more detail in Table 2.

These optical properties are used on the “cover” boundary condition for the CFD model under development. The contribution of all other wavelengths (UV and far infrared) was neglected.

c. Experimental Climate Data

The climate measurements at the greenhouse cover a timespan of around 12 days in June 2023. Five sensors logged temperature, relative humidity and the dew point every minute. The data is presented in **Figure 4**. The sensor positions are only vaguely known:

- “ambient” is somewhere outside the greenhouse
- “canopy” is inside the greenhouse at about 1.5m height
- “roof” is also inside the greenhouse, at least 50cm underneath the cover
- “soil10cm” and “soil20cm” are buried inside the greenhouse in 10cm and 20cm depth

This project has received funding from the European Union’s Horizon 2020 research and innovation program under grant agreement 101000801.

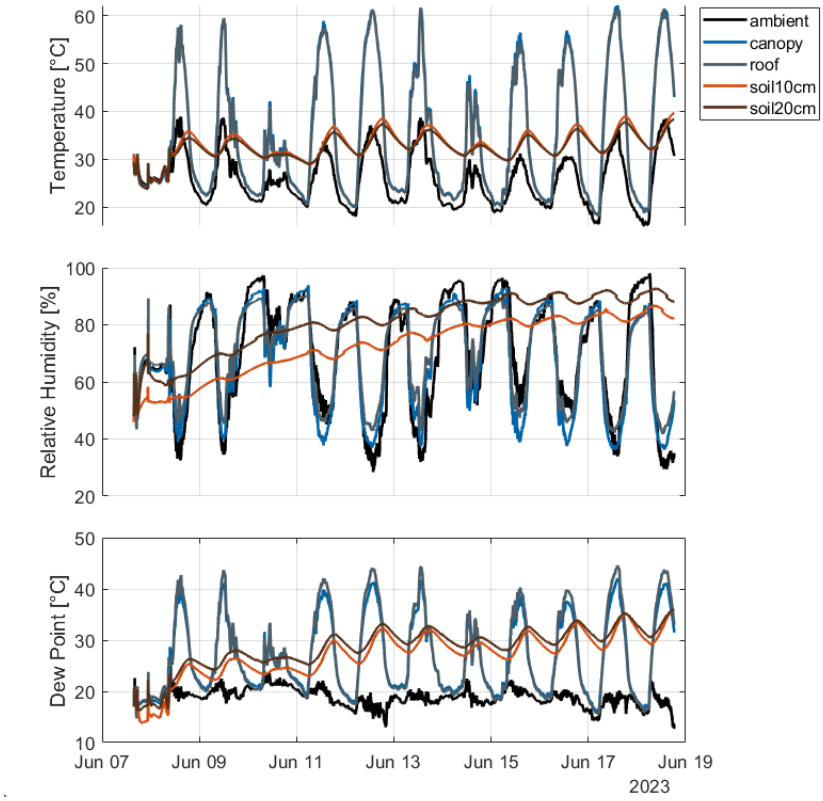

Figure 4 - The temperature, relative humidity and dew point were measured by five sensors in different positions on the greenhouse site. The data was logged every minute, starting on the 7th of June for almost 12 full days. The peaks indicate day-night-fluctuations of the local climate.

In addition, hourly data from a local weather station was collected, showing the wind speed and cloud cover as depicted in **Figure 5**.

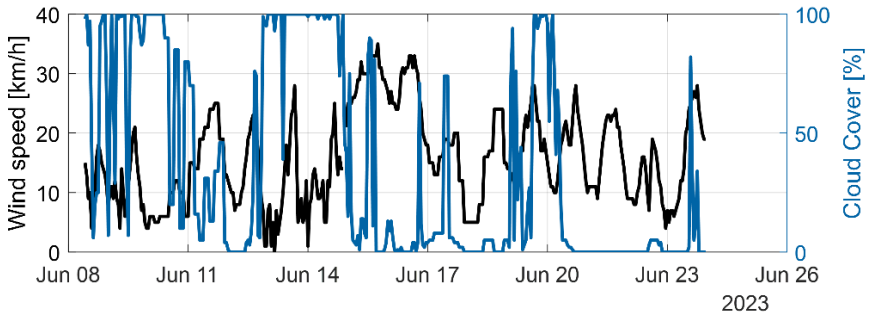

Figure 5 - Wind speed and cloud cover logged hourly by a weather station at the greenhouse site. Large variations are observed for both dimensions.

According to this data the 16th of June is selected as a reference day, as the sky is almost cloudless. On this day, two design points are selected to assess the model performance: The cool extremum is on 4:00 AM just before sunrise, and the warm extremum is 1:00 PM. At this time the air temperature within the greenhouse is coolest or warmest, respectively. The climatic procession of this day and the two chosen moments are shown in **Figure 6**.

This project has received funding from the European Union's Horizon 2020 research and innovation program under grant agreement 101000801.

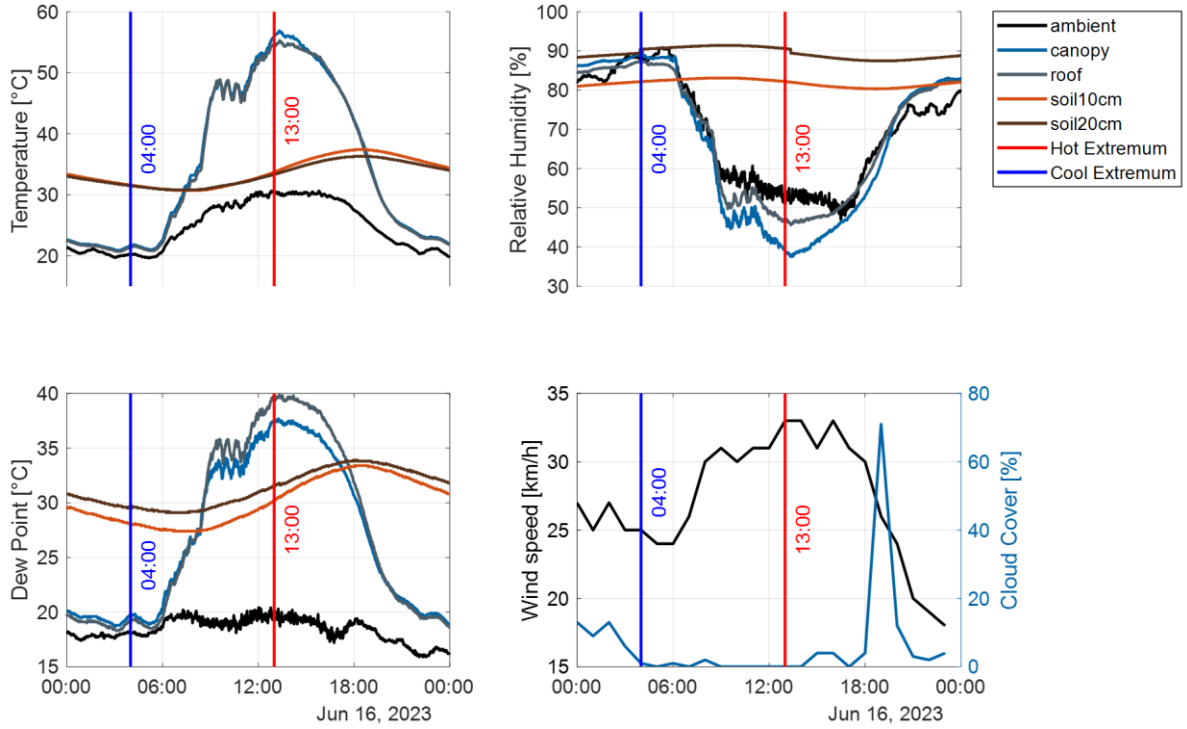

Figure 6 - Air temperature, relative humidity, and dew point inside the greenhouse on the 16th of June 2023, along with the weather data at the site on the lower right graph. The blue and red lines mark cool and warm extrema at 4:00 AM or 1:00 PM, respectively. These moments are used for conducting steady state simulations.

This project has received funding from the European Union's Horizon 2020 research and innovation program under grant agreement 101000801.

4. CFD Model

The CFD model is developed with a simplified geometry of the experimental greenhouse. Only the envelope foil with the ribs and the flat floor are considered as walls. For most of the investigations, a rib segment with adjacent symmetries is used. Finally, a simplified version of the entire test greenhouse is built in order to test the modeling approach closer to its physical equivalent.

In both models, there is no air exchange or pressure equalization with the environment, and the air-conditioning technology, the supporting structure and the plants are omitted. The problem is assessed in steady state, with a gravitational acceleration magnitude of 9.81 N/kg. The mesh, boundary conditions and material definitions are described in more detail.

a. Mesh

The simplified geometry is used to generate a structured mesh. The high-quality mesh for the reduced case with symmetry planes is shown in **Figure 7** on the left, featuring 232,148 cells. The larger mesh is shown on the right and consists of 1,778,444 cells. The cell sizes of both meshes are the result of a mesh study. The thickness of the first element on the wall is a maximum of 2mm throughout and leads to a well-resolved boundary layer with $y^+<2$ everywhere. The nodes inside the domain are a maximum of 15cm apart.

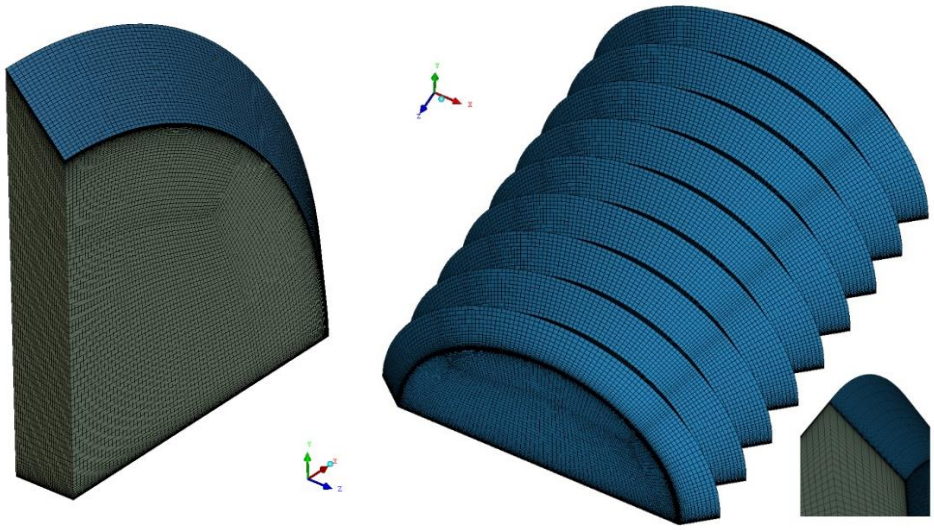

Figure 7 - The simplified mesh used for building the CFD model with symmetry planes is shown on the left. A more comprehensive model on the right is used for further investigations. The axis orientation is depicted because it is relevant for buoyancy/solar load settings, and reader orientation.

This project has received funding from the European Union's Horizon 2020 research and innovation program under grant agreement 101000801.

b. Boundary Conditions

The mesh consists of two boundary surfaces, “floor” and “cover”, for which suitable boundary conditions must be specified (symmetry planes require no further information). In Fluent, the boundary conditions are selected according to **Table 2** (with blue/red for the cool/warm extremum). The values are chosen based on measured data or assumptions described in **Section 3**.

Table 2 - Boundary conditions at the greenhouse floor and cover for the cool (blue) and warm (red) extremum

Condition	**Floor**	**Cover**
Momentum	Stationary no slip wall with standard roughness	
Thermal	Natural convection with a heat transfer coefficient α = 5/5 W/m^2/K and free stream temperature of 31/33.4°C, shell conduction through 20cm soil	Convection with α = 18/20 W/m^2/K estimated from the wind speed, and free stream temperature of 18/30.4°C, no shell conduction
Radiation	Opaque wall absorbing 90% of the direct and infrared radiation	Semi-transparent wall without absorption, transmitting 88.5% of direct visible, 18% of direct IR and 45% of diffuse hemispherical radiation
	No radiation for cool extremum	
Species	Estimated water vapor mass fraction of 0.05, assumed constant during the reference day	Relative humidity: 85/45% and mean temperature 20/55°C yield a water vapor mass fraction of 0.0012/0.0034.

c. Material Definition

The defined material properties of soil, dry air, water vapor, and humid air as a mixture of the two latter are summarized in **Table 3**. Because model is still under development and the temperature gradients are considered low, all material properties except the gas densities are defined as constants. This is an impactful simplification but considered appropriate due to the schematic nature of the current model.

Table 3 - Material used in the CFD model and their physical property settings.

Material Property	**Soil** Solid	**Dry air** Fluid	**Water vapor** Fluid	**Humid air** Species mixture
Density	1300 kg/m^3	Boussinesq-Model with 1.225 kg/m^3 reference density	Boussinesq-Model with 0.5542 kg/m^3 reference density	Volume-weighted mixing law
Specific Heat	1700 J/kg/K	1009 J/kg/K	1907 J/kg/K	Mixing-law
Thermal Conductivity	1 W/m/K	0.027 W/m/K	0.02 W/m/K	Mass-weighted mixing law
Viscosity	-	1.9 10^{-5} Pa·s	1.1 10^{-5} Pa·s	Mass-weighted mixing law
Thermal expansion coefficient	-	0.0034 1/K	0.003 1/K	-

This project has received funding from the European Union’s Horizon 2020 research and innovation program under grant agreement 101000801.

d. Other relevant Settings

Turbulence was modeled with the Realizable k-Epsilon-Model with standard wall functions because this was recommended in the preceding work (Eleftheria Vavoura, 2021). Other important solver settings are:

- The simulation is calculated with the pressure-based solver.
- Pressure and velocity are coupled, changing to SIMPLE-Coupling had no effect on the solution.
- PRESTO! spatial discretization is used for pressure.
- First order upwind discretization is used for momentum, turbulence, and energy, switching to or second order or QUICK had no effect on the solution.

5. Results and Discussion

This section presents and discusses the results from the model assessments for both the cool and warm design points. The simplified model with symmetry planes is discussed first, followed by the full greenhouse model. As the physical site is almost as long as it is wide, the assumption of symmetry will not provide precise results. Nevertheless, it is useful to assess the behavior of the different numeric models. The convergence was very good in all cases, with continuity residual being highest of all at $5 \cdot 10^{-5}$. However, the solver was unable to reduce the energy imbalance below 2.8%, indicating insufficient model assumptions affecting the energy solution.

a. Symmetric Greenhouse Model

The smaller mesh with adjacent symmetry planes is presented in this section. This model is used to conduct the mesh study, assess different solver settings such as coupling scheme, and spatial discretization methods. Different boundary conditions and modeling settings for radiation and species transport are also examined. The simulation results of the flow, the temperature field and the relative humidity are shown in **Figure 8** for the cool and warm design points.

This project has received funding from the European Union's Horizon 2020 research and innovation program under grant agreement 101000801.

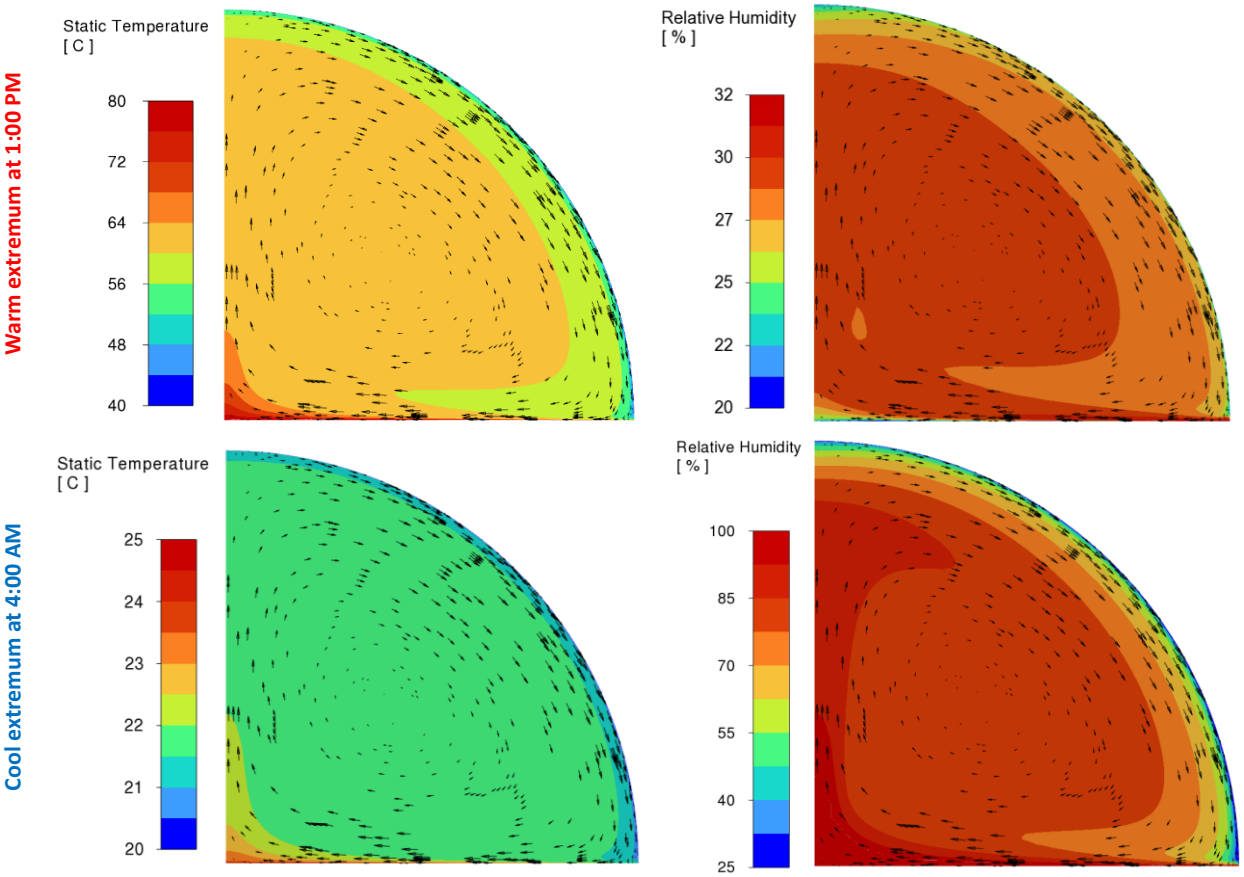

Figure 8 - Temperature and relative humidity viewed from the +z direction on the symmetry plane under the high bow for the warm (top) and cool (bottom) extremum. The velocity field is visible as proportional black arrows, the largest arrow indicating the maximum velocity of approximately 0.5/0.75m/s magnitude.

In the warm design point at 1:00 PM (see the upper two contours in **Figure 8**), the floor temperature partially rises above 100°C instead of the expected 30°C. Because the simulated solar power of around 800 W/m^2 on the greenhouse floor is realistic (Abid et al., 2023), the heat transfer to the floor is underestimated by the model. As the material properties of air and water vapor are well-known, the soil material properties were investigated further. Especially tuning the absorption coefficient of the floor showed a significant impact on the heat flux, whereas slightly changing other soil properties mainly affected the convergence history but yielded comparable solutions. Nevertheless, the fact that the floor is hotter than in the measured value is plausible because no plants were considered. In addition to the absorption of visible light through photosynthesis, the plant transpiration can account for up to 40% of the energy balance in a greenhouse (Fatnassi et al., 2023). Due to the vegetations considerable influence on the floor boundary, the absorption coefficient is not further investigated. The air temperature calculated in this way can only be validated superficially with the measured values, as the exact position of the sensors is not known. As the model overestimates the floor temperature, the measured air temperature of around 55°C is also overestimated by the simulation by approximately 5°C. The measured humidity of around 45% is correspondingly underestimated, accounting only for around 30%.

As for the cool design point at 4:00 AM (see the lower two contours in **Figure 8)**, the temperature field shows more realistic results. The solution shows air temperatures around 22°C, closely matching the measured data at the corresponding time. The simulated relative humidity also closely approaches the measured values of about 85%. This indicates that the convection coefficients estimated at the

This project has received funding from the European Union's Horizon 2020 research and innovation program under grant agreement 101000801.

boundaries and the shell conduction approach at the floor are good approximations. However, the simulated relative humidity closer to the floor occasionally exceed 100%, indicating condensation. The measurements show that temperature and dew point on canopy height are very close in the early morning. Consequentially, it is very likely that the temperature near the ground fell below the dew point during the measurements, hence leading to condensation. Again, but for different reasons, the floor boundary condition is well suited to predict the microclimate with sufficient accuracy.

b. Full Greenhouse Model

The settings found with the symmetric model are used on a more complex geometry as described in **Section 0**. Again, the cool and warm design points are taken to assess the applicability of the chosen models. As no symmetry planes are present, this model is closer to the physics involved than the symmetric model discussed before. The temperature and relative humidity fields of the converged solution are shown in **Figure 9** for the cool and in **Figure 10** for the warm design point.

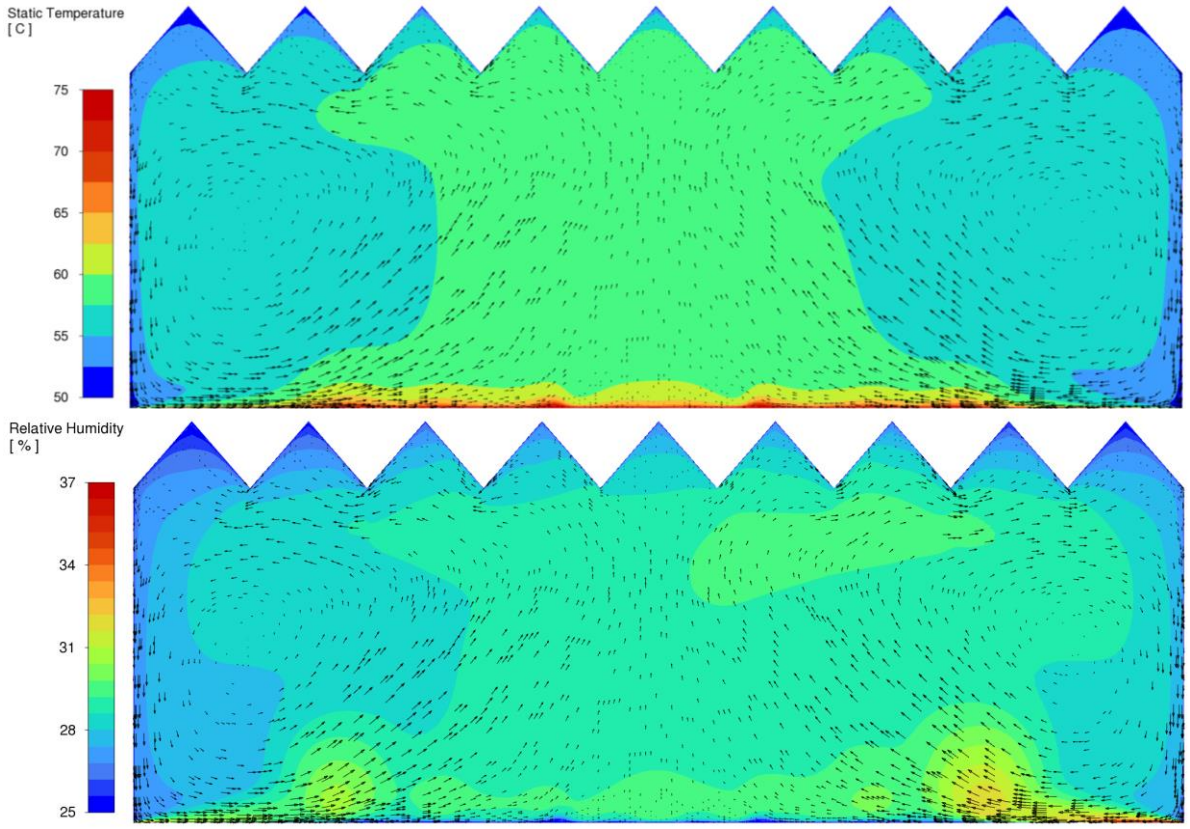

Figure 9 – Converged solution of the full greenhouse model for the warm design point at 1:00 PM. The longitudinal axis of the greenhouse is viewed from the +x direction. The temperature field (top) shows the highest temperatures on the ground, while the temperature on canopy height is around 55 to 60°C. The relative humidity (bottom) is around 30% in this area. The black arrows indicate the flow direction.

This project has received funding from the European Union's Horizon 2020 research and innovation program under grant agreement 101000801.

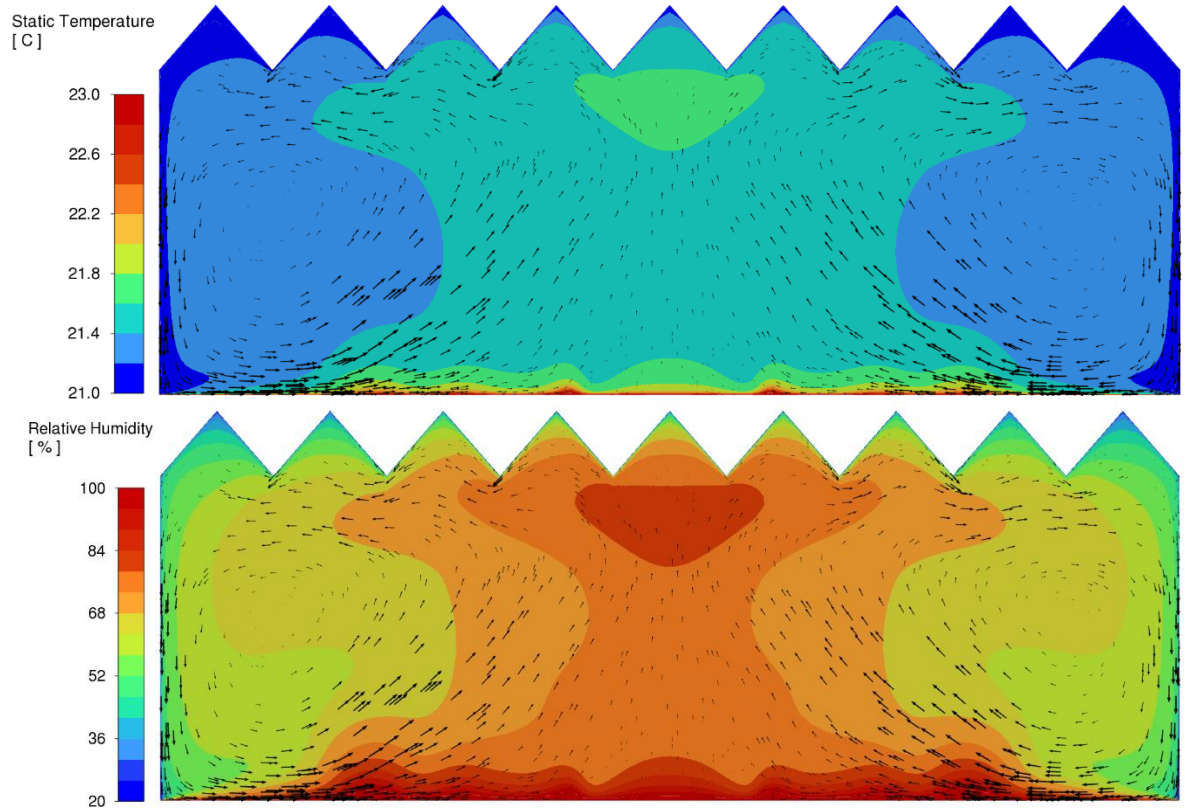

Figure 10 – Converged solution of the full greenhouse model for the cool design point at 4:00 AM. The longitudinal axis of the greenhouse is viewed from the +x direction. The top contour shows a temperature range between 20 and 25°C with small gradients. The lower contour depicts the relative humidity field, predicting around 80% in the canopy area and values above 100% near at the ground. The black arrows indicate the flow direction.

The same behavior as in the symmetric case discussed before is observed for the full model and both design points. The for the warm condition, floor temperatures partially rise above 100°C. Consequentially, the relative humidity drops below 30% instead of the expected 45% in the majority of the fluid bulk. For the cool condition, again the temperatures and relative humidities generally are in good agreement with the measurements. However, the relative humidity near the floor boundary exceeds 100%, indicating condensation phenomena that are not considered by the species model.

In contrast to the symmetrical case, the flow forms clearly visible asymmetries at both design points, illustrating the inadmissibility of symmetric simplifications. The velocity magnitudes do not exceed 1m/s, underpinning the validity of the Boussinesq Approximation for density modelling. The most significant velocity magnitudes are found above the floor, illustrating the significant influence of the vegetation not only on the heat balance, but also on the flow momentum. The flow patterns and magnitudes are shown in **Figure 11** for 1:00 PM and in **Figure 12** for 4:00 AM.

This project has received funding from the European Union's Horizon 2020 research and innovation program under grant agreement 101000801.

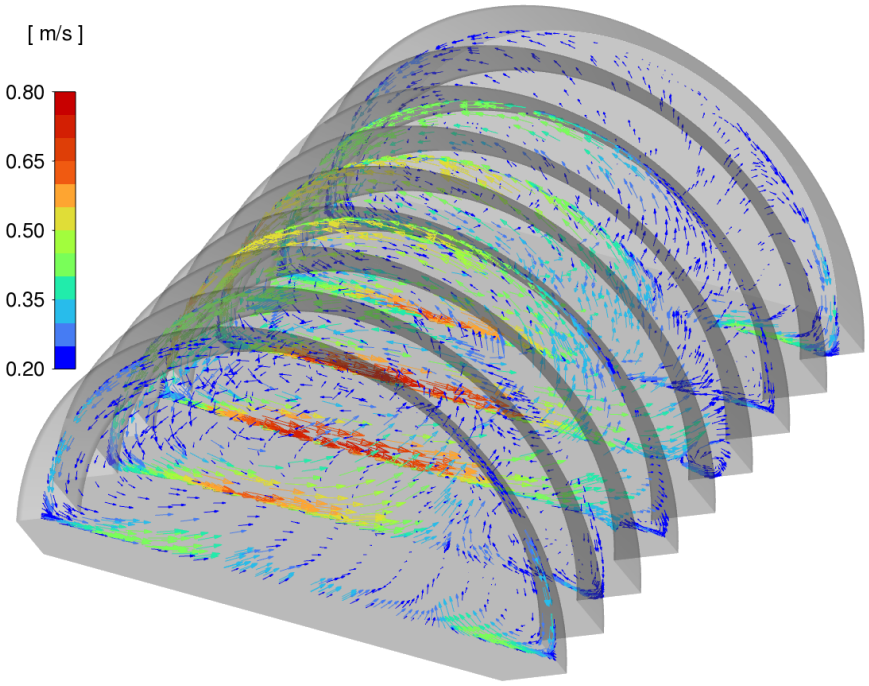

Figure 11 - The flow pattern inside the full greenhouse model for the warm design point at 1:00 PM show clear asymmetries. The highest velocity magnitudes occur close to the floor and do not exceed 0.8 m/s.

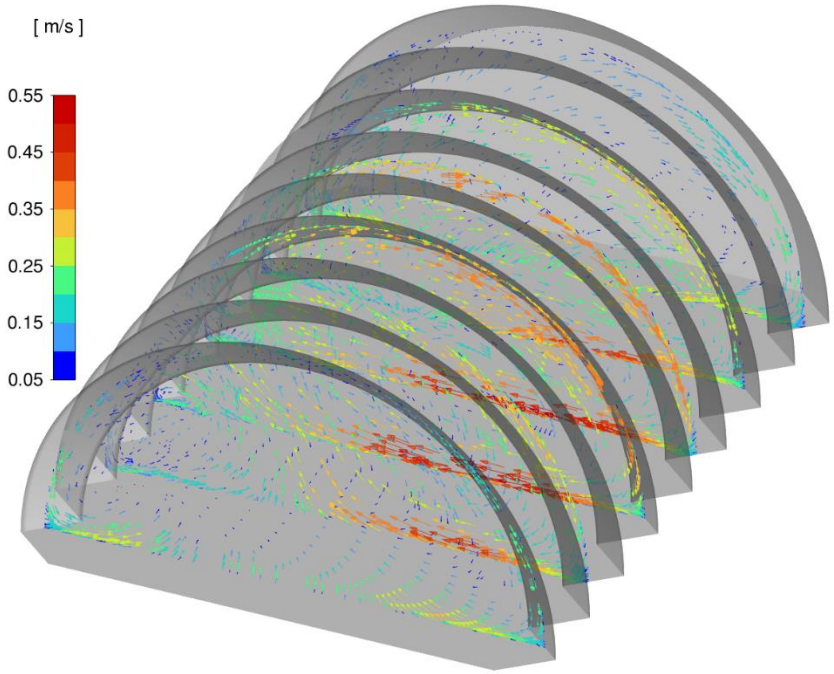

Figure 12 - The flow pattern inside the full greenhouse model for the cool design point at 4:00 AM also show clear asymmetries. The highest velocity magnitudes again occur close to the floor, but are generally lower with a maximum of 0.55 m/s.

This project has received funding from the European Union's Horizon 2020 research and innovation program under grant agreement 101000801.

6. Conclusions and Next Steps

The climate data of the experimental greenhouse in Chorfech provided a sufficient basis for the development of a CFD model. Based on the findings of the preliminary work, a simpler case with symmetry planes and a model covering the entire greenhouse were built. With the solar load model, the radiation was adapted to match the situation more accurately. Furthermore, the species transport approach was introduced for modelling air humidity. The assumptions were assessed for two sets of boundary conditions based on a cool extremum at 4:00 AM and a warm extremum at 1:00 PM.

The results clearly demonstrate that omitting the plants in the model is inadequate for both the flow calculation and the heat balances. The soil temperatures are significantly overestimated at noon, consequentially causing the relative humidity to deviate significantly from the measurements. Furthermore, a relative humidity of over 100 % above the floor can be seen for the cool design point, which indicates dew formation. However, as latent heat flows are not covered by the selected modelling approach, the energy conservation is distorted, leading to imbalances up to 3%.

The appropriate modelling of the crops, both as flow resistance and as transpiring elements, is of utmost importance to solve for accurate predictions. As these were omitted by decision, a thorough validation with the available data could not be carried out. The implementation of suitable crop models is therefore subject to further research, imposing the necessity of defining cultivation concepts.

In addition, it was found that condensation and evaporation phenomena are crucial for accurate predictions. Given the inherent complexity of such models, this subject could not be further examined with the available resources. Only after these phenomena have been included in the model, the available measurements can be utilized for a comprehensive validation.

This project has received funding from the European Union's Horizon 2020 research and innovation program under grant agreement 101000801.

7. References

Abid, H., Ketata, A., Lajnef, M., Chiboub, H., & Driss, Z. (2023). Numerical investigation of greenhouse climate considering external environmental factors and crop position in Sfax central region of Tunisia. *Solar Energy*, *264*, 112032. https://doi.org/10.1016/J.SOLENER.2023.112032

Abu-Hamdeh, N. H. (2003). Thermal Properties of Soils as affected by Density and Water Content. *Biosystems Engineering*, *86*(1), 97–102. https://doi.org/10.1016/S1537-5110(03)00112-0

ANSYS, Inc. (2023a). *Ansys Fluent Theory Guide* (Release 2023 R2).

ANSYS, Inc. (2023b). *Ansys Fluent User's Guide* (Release 2023 R2).

Eleftheria Vavoura. (2021). *D2.1 CFD Simulation in Greenhouse Farming*.

Fatnassi, H., Bournet, P. E., Boulard, T., Roy, J. C., Molina-Aiz, F. D., & Zaaboul, R. (2023). Use of computational fluid dynamic tools to model the coupling of plant canopy activity and climate in greenhouses and closed plant growth systems: A review. *Biosystems Engineering*, *230*, 388–408. https://doi.org/10.1016/J.BIOSYSTEMSENG.2023.04.016

Fenn, R. W., Shettle, E. P., Hering, W. S., & Johnson, R. W. (1981). Atmospheric optical properties and meteorological conditions. *Atmospheric Environment (1967)*, *15*(10–11), 1911–1918. https://doi.org/10.1016/0004-6981(81)90225-0

Malekjani, N., & Jafari, S. M. (2018). Simulation of food drying processes by Computational Fluid Dynamics (CFD); recent advances and approaches. *Trends in Food Science & Technology*, *78*, 206–223. https://doi.org/10.1016/J.TIFS.2018.06.006

National Institute of Standards and Technology (NIST). (2023). *Thermophysical Properties of Fluid Systems*. U.S. Secretary of Commerce. https://webbook.nist.gov/chemistry/fluid/

Ochsner, T. E. (2017). Rain or Shine. In *Rain or Shine: An Introduction to Soil Physical Properties and Processes*. Oklahoma State University Libraries. https://doi.org/10.22488/OKSTATE.21.000000

Walter Wagner. (1998). *Wärmeübertragung: Grundlagen: Vol. Kamprath-Reihe* (5th ed.). Vogel Verlag und Druck.

Wierenga, P. J., Nielsen, D. R., & Hagan, R. M. (1969). Thermal Properties of a Soil Based Upon Field and Laboratory Measurements. *Soil Science Society of America Journal*, *33*(3), 354–360. https://doi.org/10.2136/SSSAJ1969.03615995003300030009X

This project has received funding from the European Union's Horizon 2020 research and innovation program under grant agreement 101000801.